LAWRENCE
LIVERMORE
NATIONAL
LABORATORY

LLNL-JRNL-478091

Energetic stability of hydrogen-chemisorbed carbon nanotube structures

A. Maiti

April 4, 2011

Chemical Physics Letters

Disclaimer

LLNL-JRNL-478091

Energetic stability of hydrogen-chemisorbed carbon nanotube structures

A. Maiti[1]

Lawrence Livermore National Laboratory, Livermore, CA 94550, USA

To optimize the performance of carbon nanotubes in the area of hydrogen storage we explore stable structures that can form upon hydrogenation. Through free energy calculations using first-principles DFT we find that at room temperature the trans-hydride structure, *i.e.*, one in which H-atoms chemisorbed on nearest-neighbor sites alternate between outside and inside of the nanotube is the most stable structure under moderate hydrogen dosage for tubes with diameter > 1.2 nm. Such structures are energetically stable with respect to recombination into H_2 or decomposition into hydrocarbons like benzene or ethylene. We also find that the IR spectrum of the trans-hydrides display striking dependence on nanotube chirality.

Keywords: Hydrogen storage, Carbon nanotube, DFT

[1] E-mail: *amaiti@llnl.gov*

Hydrogen adsorption on carbon-based structures like graphite, nanotubes [1], activated carbon [2], and graphene [3] has generated considerable interest among researchers because of its relevance to fields as diverse as interstellar chemistry [4, 5], plasma/fusion physics [6], and most recently, hydrogen storage [7-11] and sequestration [12, 13]. In a typical storage/sequestration application H-atoms are created by the dissociation of H_2 molecules by a metal catalyst, and brought onto to a carbon (or metal-oxide) support via the spillover mechanism [9-11]. As related to storage/sequestration and the utilization of hydrogen as the energy source for fuel-cell applications it is of great interest to know the limits of the amount of hydrogen that can be stored in single-walled carbon nanotubes (SWNTs). Physisorbed H_2 interacts only weakly with nanotubes (or graphene) and should lead to very low storage levels. Thus, it is necessary to consider more stable forms, i.e., chemisorbed species [14]. Without disrupting any C-C bond of the SWNT each C-atom can accommodate one chemisorbed H, thus yielding a theoretical maximum storage capacity of $m_H/(m_H+m_C) \sim 7.7$ wt % [m_H and m_C being the atomic weight of hydrogen and carbon respectively], which is ahead of the current technology target set by the U.S. Department of Energy. Experimentally, however, most SWNTs are found to become unstable under high hydrogen dosage and decompose before reaching the theoretical maximum hydrogenation levels [15].

In order to make further progress, it is necessary to understand the most stable forms upon 100% hydrogenation, the energetics of hydrogen storage and retrieval, and possible decomposition into hydrocarbons under extreme conditions like heavy H-flux, high T, and so on. While a clearer knowledge about the atomistic structure of activated carbon is just beginning to emerge [2], most efforts in the literature have centered on carbon

nanotubes and graphene. Interestingly, most recent discussions on this have focused on all H-atoms being on one side of the absorbing surface [14-17], i.e., top of a graphene sheet, or exterior wall of a SWNT, etc. The physical justification behind this is the high energy barrier for a H-atom to cross the graphene plane (or a SWNT wall). However, given that the stability comparison here is with respect to high-energy processes like C-C bond-scissioning into hydrocarbon formation, it is also important to bring back into discussion structures that involve chemisorbed H simultaneously on both sides [18, 19].

In this Letter we consider two different hydride structures, i.e., SWNTs with all H-atoms chemisorbed on the outside wall (referred to below as SWNT-exo-hydride) and ones with H-atoms on neighboring C-atoms alternating between outside and inside walls (henceforth referred to as SWNT-trans-hydride), and explore their relative energetic stability with respect to recombination into H_2 and possible decomposition products involving hydrocarbons. We also investigate how such stability varies as a function of tube diameter and chirality. Structures in which all H-atoms are on the inside wall of the SWNT are energetically unstable and not considered in this work.

The pristine SWNTs and SWNT-hydrides in this work were represented by periodic supercell models with the nanotube aligned along the *z*-axis. The cell-length in this direction was made equal to the smallest repeat-unit of the SWNT in order to represent an effectively infinite tube, while the cell-lengths in the *x* and *y* directions were made large enough (30 Å or greater) to ensure negligible transverse interactions among the periodic images. For graphene, a periodic repeat unit of its basal plane was aligned along the *x*-*y* plane with images normal to the plane separated by a 30 Å vacuum slab. Geometry optimization and harmonic frequency calculations were then performed using the

periodic Density Functional Theory (DFT) code DMol^3 [20]. The electronic wave functions were expanded in a double-numeric polarized (DNP) basis set represented on a "medium" numerical grid. The gradient-corrected PBE exchange-correlation functional [21] was employed in all calculations, and accurate Brillouin-zone sampling ensured through the summation over a finite set of K-points chosen according to the Monkhorst-Pack scheme [22] with a grid spacing of 0.05 Å^{-1}.

Four nanotube systems and their hydrides were explored in this study, *i.e.*, (3, 3), (5, 5), (10, 0), and graphene. Fig. 1 displays the geometry-optimized structures of the exo-hydride and the trans-hydride of three of these systems, *i.e.*, (3, 3), (5, 5), and graphene. Clearly chemisorbed H lead to very different structural relaxations in the exo- and trans-hydrides. For graphene, the C-atoms in the exo-hydride are in a perfect plane, isotropically expanded by ~ 19 % relative to pristine graphene. For large-diameter SWNT-exo-hydrides this translates into perfectly circular cross-section, with both diameter and length elongated by ~ 19% relative to the pristine SWNT. The trans-hydride of graphene, on the other hand, is a puckered structure with a net cell-parameter expansion of only ~ 4% relative to graphene, and leads to a puckered cross-section of the SWNT-trans-hydrides with generally much less elongation in length and diameter as compared to the exo-hydride. For narrower SWNTs (d < 1 nm) the fractional expansion of length and diameter in both hydrides show some dependence on the nanotube diameter and chirality. Due to puckering all C-atoms in the trans-hydride have near-perfect sp^3 coordination. In contrast, the smooth curvature of the exo-hydride surface results in a less-ideal coordination (except for very narrow tubes), thereby making such hydrides energetically less stable (see discussion below). With all valence electrons tied up in C-C

or C-H σ-bonds both hydride structures are electrical insulators, with a higher band-gap for the sp^3-coordinated trans-hydride. This is indeed borne out in electronic band-structure analysis [18, 19].

Besides optimized structures, two sets of properties were noted from the DMol^3 calculations: (1) the total energy (E) of each geometry-optimized structure, and (2) the vibrational frequencies ν_j {j = 1, 2, …, $3N$}, where N is the number of atoms in the computational cell. The total Helmholtz free energy (F) was then computed for each structure using to the standard formula:

$$F = E + \sum_j \frac{1}{2} h\nu_j + \sum_j \frac{h\nu_j}{\exp(h\nu_j / k_B T) - 1}, \qquad (1)$$

where T is the absolute temperature, and h and k_B are the Planck's constant and the Boltzmann constant respectively. The second term on the right hand side (RHS) of eq. (1) represents the zero-point energy contribution while the last term represents the vibrational free energy at finite temperature.

Table 1 displays the DMol^3 results for the total energy (normalized per CH pair) of the four nanotube systems for the two types of hydrides (exo- and trans-) and compares to the case in which H_2 molecules are physisorbed on the corresponding pristine SWNT (SWNT + H_2 (1:1)). To compare the energetic stability of these nanotube systems relative to common hydrocarbons, we also performed similar DMol^3 calculations for four additional molecules, i.e., methane, ethane, ethylene, and benzene (with an appropriate number of H_2 subtracted so as to maintain a C:H ratio of 1:1). These systems are represented in the last four rows of Table 1. From a comparison of the normalized total

energy the methane system turns out to be the most stable, which is to be expected given the highest number of C-H bonds in such system. Table 1 expresses all total energies relative to this methane system, i.e., through the quantity ΔE, as listed in column 2. To visualize the relative stability of all these structures Fig. 2 (top) plots the quantity ΔE as a function of the inverse nanotube-diameter d ($1/d = 0$ for graphene), from which we note the following results: (1) the energetic stability of both hydrides (as well as pristine SWNTs) are functions of tube-diameter only, and has only a weak dependence on chirality; (2) the trans-hydride is always more stable with respect to recombination into H_2, and its stability increases with tube diameter; (3) the stability of the exo-hydride shows exactly the opposite behavior, *i.e.*, decreases with increasing d; such hydrides are energetically more stable than the trans-hydride only for the narrowest of tubes with $d <$ 0.45 nm; (4) for $d > 0.8$ nm, the trans-hydride is even more stable than Benzene, the most stable (small) hydrocarbon with a C:H ratio of 1:1. Other possible (1:1) products, e.g., (trans) poly-acetylene or ethylene ($- H_2$) are energetically less stable than benzene. Thus for not-too-high H-dosages, the trans-hydride appears to be the most stable chemisorbed structure possible. However, very high H-dosages can potentially lead to nanotube decomposition into small alkanes, as is evident from the ethane and methane energies being tens of kcal/mol lower in all cases.

The above analysis is based only on the total energy and does not take into account any thermodynamic considerations, which could be important given the small energy differences between various structures. To this end, column 4 of Table 1 lists the vibrational free energy of each structure at room temperature (300 K), which is the sum of the last two terms on the RHS of eq. (1), with the zero-point contribution (the middle

term of the RHS of eq. (1)) listed separately in column 3. Clearly for all systems the zero-point energy constitutes a significant contribution to the room-temperature free energy. Column 4 represents the Helmholtz free energy (ΔF) normalized per CH and expressed relative to the most stable, *i.e.*, the methane system. Fig. 2(bottom) is a stability plot based on ΔF. Although qualitatively it is similar to Fig. 2(top), some quantitative differences are noticeable: (1) the stability of the trans-hydride relative to the physisorbed structure SWNT + H_2 (1:1) becomes worse. For large diameters (graphene end) the trans-hydride is stable only by 2.5 kcal/mol (as compared to 5.7 kcal/mol stability in Fig. 2(top)), while the physisorbed structure becomes more stable at $d < 0.5$ nm; (2) the trans-hydride becomes more stable than benzene for $d > 1.2$ nm (as compared to $d > 0.8$ nm in Fig. 2(top)); and (3) the relative stability of exo- and trans-hydrides is similar to that in Fig. 2(top), with the crossover still predicted at $d \sim 0.45$ nm.

As a potential experimental characterization tool to distinguish the two hydrides, we computed the Infrared (IR) spectrum for both hydride species for a (5, 5) and a (10, 0) tube. Although DMol[3] can calculate vibrational frequencies, the IR intensity calculation has not been implemented under periodic boundary conditions. Instead of switching to a different DFT code that can accomplish this through a linear response or a Berry phase approach [23, 24] we adopted a computationally less expensive classical force field based method. The IR calculations reported here employed a state-of-the-art class II force field, COMPASS [25] and were performed on structures periodically extended along the nanotube length, each consisting of 320 atoms. These results, displayed in Fig. 3, show that both for armchair and zigzag tubes the IR spectra for the two hydrides show substantial differences. In particular, it is interesting to analyze the highest frequency C-H

stretch modes, which for both trans-hydrides get blue-shifted by ~ 100-150 cm^{-1} (relative to the corresponding exo-hydride), and in addition get split into two distinct peaks separated by 35-40 cm^{-1}. Animation of the split modes reveals that for the (10, 0) tube the higher-frequency mode represents C-H stretch involving primarily the inner H-atoms, while the lower-frequency split mode involves C-H stretch of the outer H-atoms. For the (5, 5) armchair tube exactly the opposite happens, i.e., the upper split mode involves the outer atoms, while the lower mode involve the inner atoms.

Finally we address the question of whether the SWNT-trans-hydride can actually form, and if so, what are the plausible pathways. To provide some insight, it is instructive to ask the following question: given a H-atom already chemisorbed on a C-site, what would be the most stable chemisorption site for a second H-atom? Recent DFT calculations [16] suggest that the answer is a neighboring C-atom (the most stable is the para neighbor closely followed by the nearest or ortho neighbor), as we have also verified from $DMol^3$ calculations. However, flipping an ortho H-neighbor to the other side leads to an additional energetic stability of 15 kcal/mol. Thus, if C-atoms are allowed to access both surfaces (either through diffusion or direct impingement), it should start the spontaneous nucleation of the trans-hydride structure. The access to both surfaces can possibly happen through "end-on" contacts of SWNT to catalytic metal particles [9] or through the presence of defects like vacancies [26], which can provide low-energy pathways through the nanotube surface. The free energy landscape of the subsequent addition of H-atoms to ultimately create the trans-hydride has recently been investigated with DFT calculations [27, 28]. Such works show that for the first few atoms the process is endothermic with respect to physisorbed H_2 molecules on the nanoube surface.

However, once a critical-sized nucleus forms, the process becomes exothermic and should self-sustain. Considering that H_2 molecules may need to be broken down by transition metal catalysts, one also needs to consider the migration kinetics of the resulting H radicals over the metal and the already-chemisorbed H sites. Some work toward that end has appeared in the recent literature [29].

Acknowledgement: This work was performed under the auspices of the U.S. DOE by Lawrence Livermore National Laboratory under Contract DE-AC52-07NA27344.

References:

1. S. Iijima, *Nature* **354** (1991) 56.
2. P. J. F. Harris, Z. Liu, K. Suenaga, *J. Phys. Condens. Matter.* **20** (2008) 362201.
3. K. S. Novoselov et al., *Science* **306** (2004) 666.
4. S. Cazaux, A. Tielens, *Astrophys. J.* **604** (2004) 222.
5. T. Henning, F. Salama, *Science* **282** (1998) 2204.
6. G. Federici *et al.*, *Nucl. Fusion* **41** (2001) 1972.
7. A. C. Dillon, M. J. Heben, *Appl. Phys. A* **72** (2001) 133.
8. A. G. Lipson, B. F. Lyakhov, E. I. Saunin, A. Y. Tsivadze, *Phys. Rev.* B **77** (2008) 081405.
9. Y. Li, R. T. Yang, *J. Am. Chem. Soc.* **128** (2006) 8136.
10. A. D. Lueking, R. T. Yang, *Appl. Catal. A* **265** (2004) 259.
11. L. Wang, R. T. Yang, *Energy Environ. Sci.* **1** (2008) 268.
12. A. Maiti et al., *Chem. Phys. Lett.* **475** (2009) 223.
13. A. Maiti, R. Gee, R. Maxwell, and A. Saab, *J. Phys. Chem. B* **110** (2006) 3499.
14. A. Nikitin et al., *Phys. Rev. Lett.* **2005**, *95*, 225507.
15. A. Nikitin, X. Li, Z. Zhang, H. Ogasawara, H. Dai, A. Nilsson, *Nano Lett.* **8** (2008) 162.
16. L. Hornekær *et al.*, *Phys. Rev. Lett.* **96** (2006) 186102.
17. L. Hornekær *et al*., *Phys. Rev. Lett.* **96** (2006) 156104.

18. J. Li, T. Furuta, H. Goto, T. Ohashi, Y. Fujiwara, S. Yip, *J. Chem. Phys.* **119** (2003) 2376.

19. O. Gulseren, T. Yildirim, S. Ciraci, *Phys. Rev. B* **66** (2002) 121401.

20. B. Delley, *J. Chem. Phys.* **113** (2000) 7756.

21. J. P. Perdew, K. Burke, M. Ernzerhof, *Phys. Rev. Lett.* **77** (1996) 3865.

22. H. J. Monkhorst, J. D. Pack, *Phys. Rev. B* **13** (1976) 5188.

23. A. Painelli and Z. G. Soos, *Chem. Phys.* **325** (2006) 48.

24. R. Resta, *J. Phys: Cond. Mat.* **14** (2002) R625.

25. H. Sun, *J. Phys. Chem. B* **102** (1998) 7338.

26. Andzelm, J.; Govind, N; Maiti, A. *Chem. Phys. Lett.* **421** (2006) 58.

27. Y. Lin, F. Ding, B. I. Yakobson, *Phys. Rev. B* **78** (2008) 041402(R).

28. A. Bilić, J. D. Gale, *J. Phys. Chem. C* **112** (2008) 12568.

29. A. J. Du, S. C. Smith, X. D. Yao, G. Q. Lu, *J. Am. Chem. Soc.* **129** (2007) 10201.

Table 1. DFT-computed total energy (ΔE) at T = 0 K, vibrational free energy contribution at 300 K, and the net Helmotz free energy (ΔF) at 300 K for various nanotube systems and their hydrides. Also shown explicitly is the contribution of the zero-point energy. ΔE and ΔF are expressed relative to the most stable (i.e. Methane – 3/2 H_2) system. All systems possess a C:H ratio of 1:1 and all energies are normalized per CH unit.

System	ΔE (T = 0 K) (kcal/mol/CH)	Vibrational Free Energy (kcal/mol/CH)		ΔF (T = 300 K) (kcal/mol/CH)
		Zero-point energy	T = 300 K*	
Graphene + H_2 (1:1)	30.5	7.4	9.2	23.1
Graphene-exo-hydride	65.5	13.7	14.2	63.1
Graphene-trans-	24.8	12.0	12.3	20.6
(10, 0) SWNT + H_2	34.0	7.4	9.2	26.6
(10, 0)-exo-hydride	46.1	12.5	12.9	42.4
(10, 0)-trans-hydride	28.7	12.3	12.6	24.7
(5, 5) SWNT + H_2	34.9	7.4	9.2	27.5
(5, 5)-exo-hydride	43.8	11.6	12.0	39.2
(5, 5)-trans-hydride	30.3	11.6	11.9	25.7
(3, 3) SWNT + H_2	42.4	7.4	9.2	35.0
(3, 3)-exo-hydride	34.1	12.0	12.4	29.9
(3, 3)-trans-hydride	41.9	12.9	13.2	38.5
Benzene	28.6	10.2	10.9	22.9
Ethylene – H_2	30.1	12.2	12.6	26.1
Ethane – H_2	10.7	16.1	15.1	9.2
Methane – 3/2 H_2	0.0	17.5	16.6	0.0

*Includes zero-point energy

Figure Captions:

Fig. 1. (top row) DFT-optimized exo-hydride structures of armchair SWNTs (3, 3), (5, 5), and graphene; (second row) corresponding trans-hydrides.

Fig 2. Graphical representation of the data in Table 1 plotted as a function of the inverse of SWNT pristine diameter (d). (top) ΔE (Table 1, column 2); (bottom) ΔF at T = 300 K (Table 1, column 5). See text and the caption of Table 1 for more details.

Fig. 3. Computed IR spectra of exo- and trans-hydrides of (5, 5) armchair and (10, 0) zigzag SWNTs.

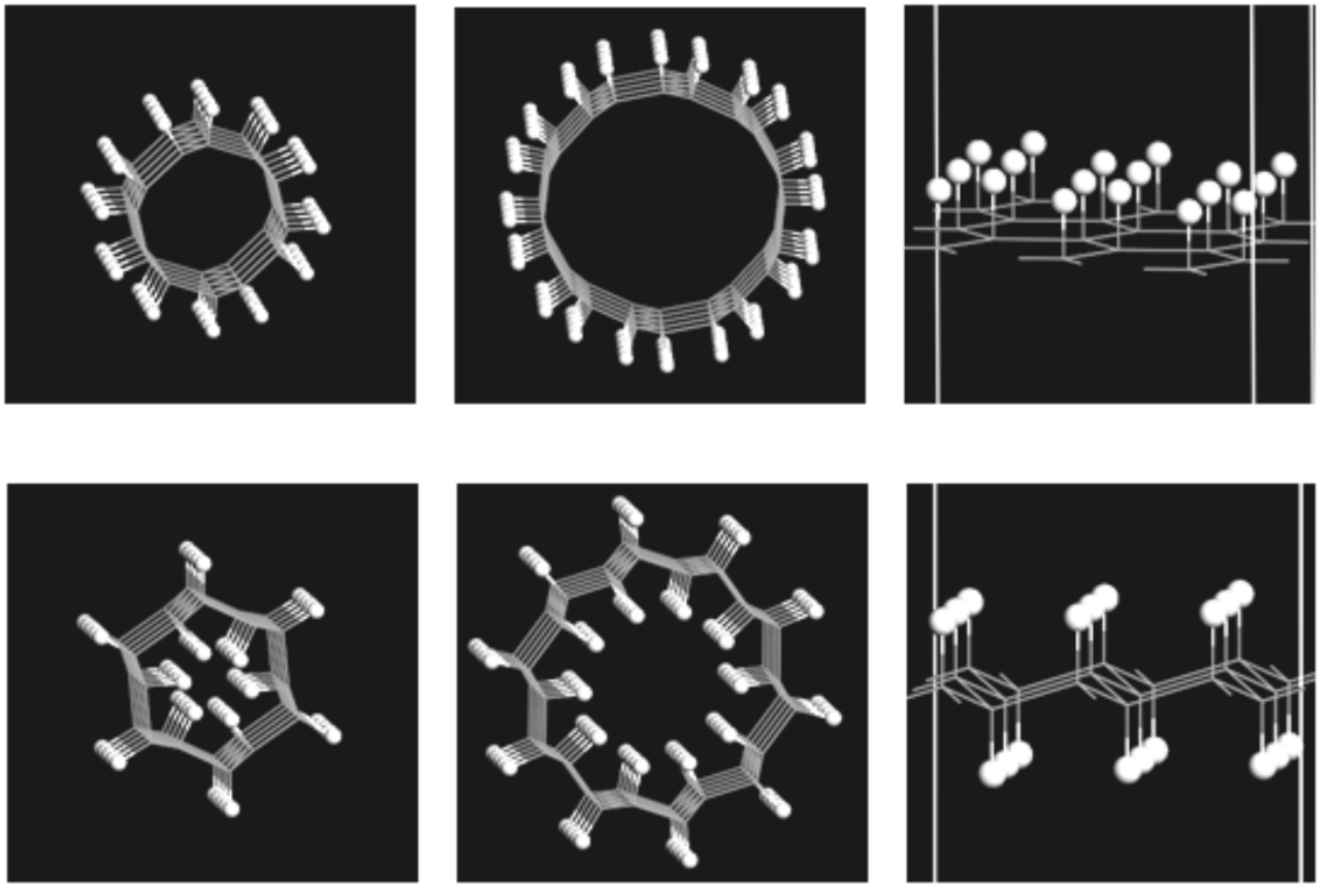

Figure 1

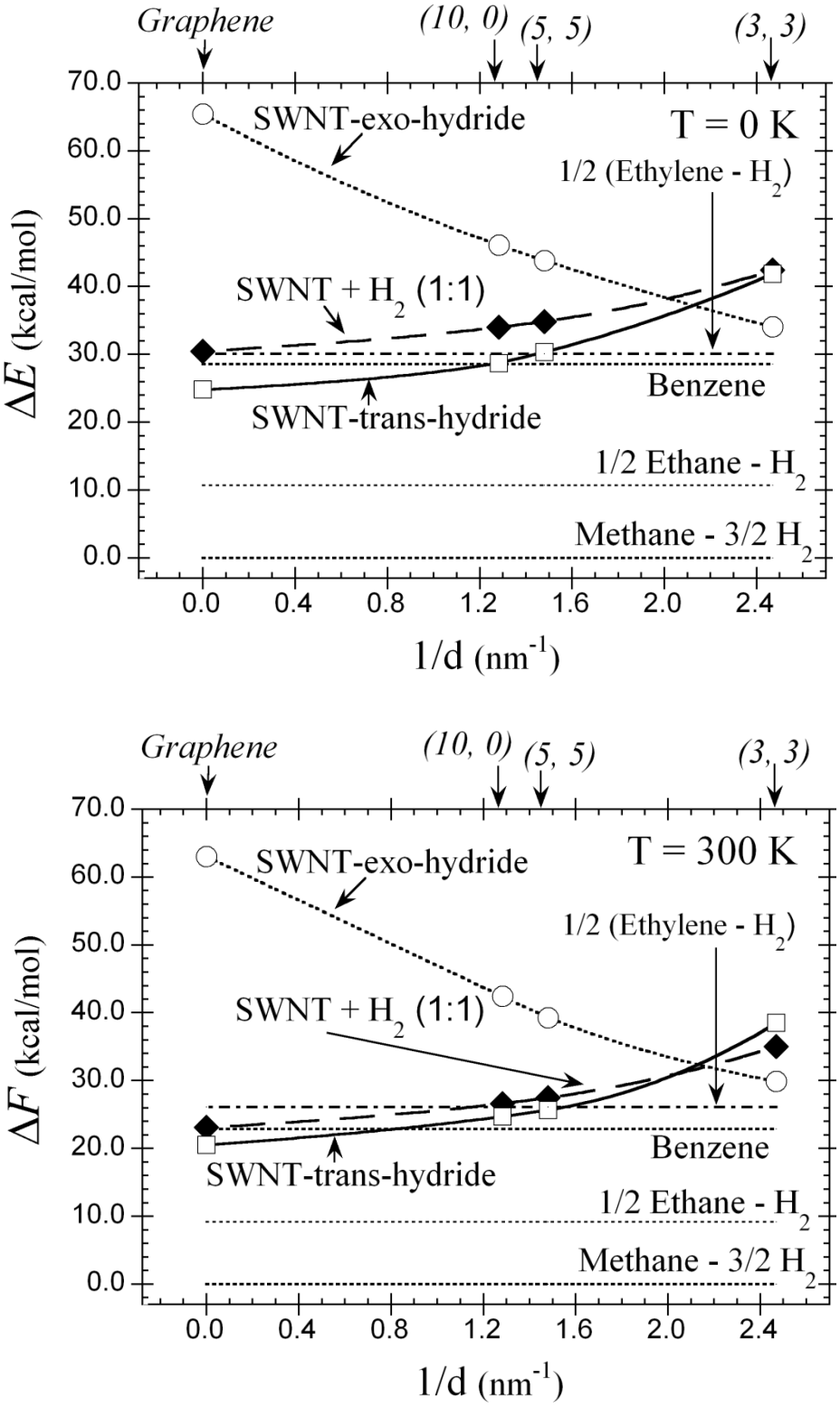
Graphene
(10, 0)
(5, 5)
(3, 3)
SWNT-exo-hydride
T = 0 K
1/2 (Ethylene - H2)
SWNT + H2 (1:1)
Benzene
SWNT-trans-hydride
1/2 Ethane - H2
Methane - 3/2 H2
ΔE (kcal/mol)
1/d (nm-1)
T = 300 K
ΔF (kcal/mol)

Figure 2

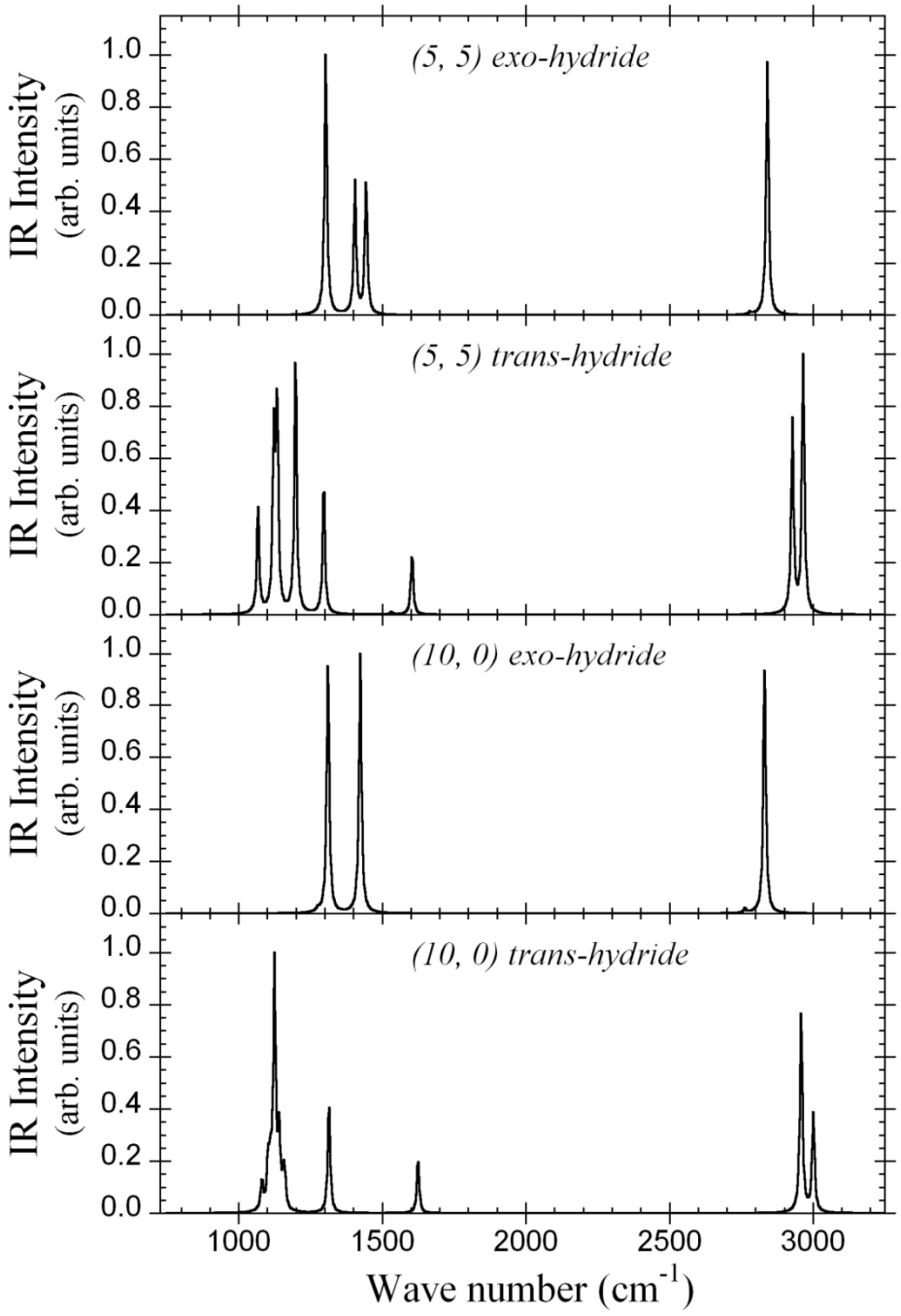
(5, 5) exo-hydride
(5, 5) trans-hydride
(10, 0) exo-hydride
(10, 0) trans-hydride
IR Intensity
(arb. units)
0.0
0.2
0.4
0.6
0.8
1.0
1000
1500
2000
2500
3000
Wave number (cm-1)

Figure 3